

## Electro-optic detection of Bloch oscillations

T. Dekorsy,<sup>1</sup> P. Leisching,<sup>1</sup> K. Köhler,<sup>2</sup> and H. Kurz<sup>1</sup>

<sup>1</sup>Institut für Halbleitertechnik, Rheinisch-Westfälische Technische Hochschule Aachen, D-52056 Aachen, Germany

<sup>2</sup>Fraunhofer-Institut Für Angewandte Festkörperphysik, D-79108 Freiburg, Germany

The coherent motion of electronic wave packets in the Wannier-Stark regime of externally biased GaAs/Al<sub>x</sub>Ga<sub>1-x</sub>As superlattices is investigated by a time-resolved electro-optic technique. As predicted by the semiclassical theory, electronic wave packets undergo Bloch oscillations. They are observed via anisotropic changes in the refractive index associated with an intraband polarization, which is set up by the coherent spatial motion of electronic wave packets relative to localized holes. The oscillation amplitude depends strongly on the initial excitation conditions. Frequency, amplitude, and dephasing of Bloch oscillations are investigated over a wide range of electric fields. Complementary results to four-wave mixing and THz emission experiments are obtained.

The optical excitations of coherent excitonic wave packets and the study of their dephasing in semiconductor heterostructures using femtosecond time-resolved optical techniques is a subject of great current interest.<sup>1</sup> Recently, the excitation of coherent wave packets performing Bloch oscillations (BO's) in GaAs/Al<sub>x</sub>Ga<sub>1-x</sub>As superlattices (SL's) has been demonstrated.<sup>2-4</sup> The optically controlled coherent superposition of several Wannier-Stark (WS) transitions<sup>5</sup> creates a nonstationary wave packet in a biased SL. In close analogy to semiclassical BO's in solid state,<sup>6,7</sup> the electronic wave packets perform oscillations in real and *k* space under the combined influence of a periodic potential of the SL and a static potential applied.<sup>8</sup> The first evidence for the existence of BO's in four-wave mixing (FWM) experiments is the fact that the frequency  $\nu$  can be tuned by the applied electric field *F* according to  $\nu = eFd/h$ , where *d* is the SL period and *h* Planck's constant. Evidence for the oscillation of the wave packet in space is drawn from the observation of coherent THz emission.<sup>4</sup>

Here, we demonstrate an experimental method, which enables the direct detection of the *internal* polarization in the SL setup by the spatial wave-packet oscillations. Transmittive electro-optic sampling (TEOS) is based on the detection of the optical anisotropy induced by a macroscopic polarization  $P_z(t)$  via the linear electro-optic effect. TEOS probes directly the amplitude and phase of BO's and with that the source of the THz emission.

In the present paper, we would like to emphasize the specific difference between the modulation of the *interband* and *intraband* polarizations arising from the nonstationary wave packets initially generated. In FWM experiments, a modulation of the interband polarization with the Bloch frequency is detected. In THz and TEOS experiments, however, the dipole moment set up by the spatial oscillations of the electronic wave packets alone is detected, when the holes can be assumed as localized in weak electric fields. From this point of view, we also expect distinct differences in the dephasing times determined in FWM and TEOS experiments. The dephasing of the interband polarization in FWM depends on the loss of coherence of excitons, while in experiments sensitive to the intraband polarization such as TEOS the dephas-

ing should be mainly governed by the loss of coherence of the electronic subsystem alone.

In addition to the difference in the interband and intraband dynamics, specific differences in the experimental techniques employed for the investigation of BO's have to be considered. In THz emission experiments, the emission from the intraband polarization is detected in the far field by a dipole antenna with a time resolution of  $> 250$  fs. In FWM, BO's are observed as a modulation of the third-order interband polarization that decays with  $T_2/2$  (Ref. 9) of about 1 ps at low temperatures for our sample and excitation conditions. Thus beating phenomena with periods larger than this interband  $T_2$  cannot be detected. Since TEOS is not restricted by the interband  $T_2$  and has the time resolution of the temporal width of the probe pulse, it offers significant complementary information on the dynamics of BO's compared to FWM and THz-emission experiments.

The equivalence of semiclassical BO's and the quantum mechanical description of coherently superposed WS states has been shown recently.<sup>10</sup> Here, we will not discuss this analogy in detail and keep the established terminology of BO's for quantum beats in the Wannier-Stark regime of a biased SL. However, an important parameter in the WS picture is the localization length *L* given by  $L \approx \Delta/eF$ , where  $\Delta$  is the width of the miniband. For high fields, the wave function is localized in a single well ( $L < d$ ). As a consequence, spatial indirect WS transitions disappear. Therefore, the amplitude of BO's should depend strongly on the localization length of the WS states involved, that is equivalent to the semiclassical real-space amplitude of BO's. Thus the amplitude of the intraband polarization observed in TEOS experiments should decrease at higher fields.

In a SL composed of 43*m* symmetry group material such as GaAs and Al<sub>x</sub>Ga<sub>1-x</sub>As, an oscillating macroscopic polarization induces birefringence, which is detected in a pump-probe setup with a circularly polarized probe beam.<sup>11</sup> The anisotropic phase retardation within the sample causes the transmitted probe beam to become elliptically polarized. The degree of ellipticity is measured in difference detection by subtraction of the intensity of the probe beam along the two main axes of the ellipse via a polarizing beam splitter (Fig.

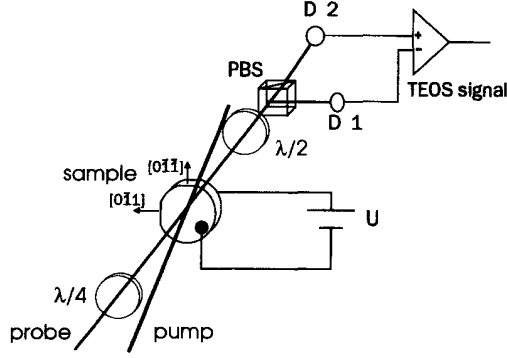


FIG. 1. Experimental setup for transmittive electro-optic sampling (TEOS) experiments. PBS denotes a polarizing beamsplitter,  $D1$  and  $D2$  are photodetectors.

1). A similar technique has been applied for the observation of transient surface fields<sup>12</sup> and coherent LO phonons<sup>13</sup> in a reflection geometry. For mapping the internal field dynamic in the SL, we prefer the transmission instead of a reflection geometry in order not to detect field changes at one side of the SL only. In the low field limit, the TEOS signal is linear proportional to the electric field changes  $\Delta F_z(\tau)$  in the SL perpendicular to the growth direction:<sup>11</sup>

$$\Delta T_{eo}(\tau)/T_0 = (4\pi/\lambda)n_0^3 r_{41} \Delta F_z(\tau)l, \quad (1)$$

where  $T_0$  is the transmitted intensity,  $\tau$  is the time delay,  $\lambda$  the wavelength,  $n_0$  the refractive index,  $r_{41}$  the electro-optic coefficient, and  $l$  the thickness of the SL. Since the probe is at the wavelength of optical resonances of the SL, the  $R_{41}$  and  $n_0$  will be subject to dispersion. The optical pulse is energetically much broader (22 meV) than the WS transitions involved, thus the pulse averages over the dispersion of the electro-optic coefficient, which will therefore not be considered further. *Isotropic* transmission changes due to phase-space filling of the involved transitions should not contribute to the *anisotropic* TEOS signal.

In the first approximation the electric field changes are related to the dynamics of the coherent wave packet via

$$\Delta F_z(\tau) = (1/\epsilon\epsilon_0)Ne\langle\Delta z_e(\tau)\rangle, \quad (2)$$

where  $\langle\Delta z_e(\tau)\rangle = \langle\Psi_{WS}^*(\tau)|z|\Psi_{WS}(\tau)\rangle$  is the relative displacement of the coherent WS wave packet  $\Psi_{WS}$  relative to the localized hole and  $N$  the excitation density. By applying a highly sensitive real-time data-acquisition system, in which the time delay is achieved via a retroreflector mounted onto a speaker shaker, relative transmission changes in the order of some  $10^{-7}$  can be detected with 10 min signal averaging.<sup>14</sup> Taking a value for the electro-optic coefficient  $r_{41}$  at the band edge of GaAs of  $1.5 \times 10^{-10}$  cm/V,<sup>15</sup> a wavelength of  $\lambda = 800$  nm, an electro-optic active length of  $1 \mu\text{m}$ , and a refractive index of 3.4, we estimate the lower detection limit in  $\Delta F_z$  to be 1 V/cm. This limit may be lower due to enhancement of the electro-optic coefficient at resonances or when the frequencies approach the optical phonon frequency.<sup>16</sup>

The SL consists of 35 periods of 97 Å wide GaAs wells and 17 Å wide  $\text{Al}_{0.7}\text{Ga}_{0.3}\text{As}$  barriers embedded in  $\text{Al}_{0.7}\text{Ga}_{0.3}\text{As}$  buffers. It is externally biased via an Ohmic contact on the  $n$ -doped substrate and a semitransparent Cr/Au Schottky contact on top of the sample. For transmis-

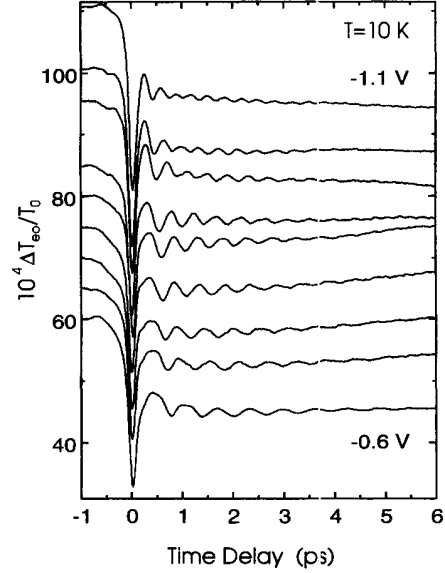


FIG. 2. TEOS signals for different applied voltages in the Wannier-Stark regime of the superlattice at an excitation density of  $2 \times 10^9$  cm<sup>-2</sup>. The curves are shifted proportional to the voltage applied.

sion measurements, the substrate has been partially removed by wet etching. The sample is positioned in a cryostat and the measurements are performed at 10 K. For the lowest electronic (heavy-hole, light-hole) miniband a width of 19 meV (1.9 meV, 18 meV) is calculated using the Kronig-Penney model. The narrow heavy-hole miniband width leads to a strong localization of the heavy-hole wave functions even at weak electric fields. The WS ladder in this sample is characterized by absorption and reflectance spectra under the same excitation conditions as in the time-resolved experiment.<sup>4,17</sup> The same sample has also been used for the investigation of BO's in THz emission<sup>4</sup> and FWM experiments.<sup>3,17</sup> The laser source is a Kerr-lens mode-locked Ti-sapphire laser with 150 fs pulse width and a spectral width of 22 meV.

Figure 2 depicts TEOS signals for different reverse bias voltages between  $-0.6$  V and  $-1.1$  V applied to the SL at an excitation density of  $2 \times 10^9$  carriers per well and cm<sup>2</sup>. The curves are shifted vertically proportional to the applied voltage. The laser is centered at 805 nm, thus covering the heavy hole 0 to electron  $-1$  ( $hh_{-1}$ ) transitions and heavy hole 0 to electron 0 ( $hh_0$ ) transitions of the WS ladder over the range of electric fields depicted. At these electric fields and laser energy the light-hole transitions can be neglected. They are separated by about 11 meV from the  $hh_{-1}$  transitions and exhibit only a third of the absorption strength compared to the  $hh$  transitions. The TEOS signals in Fig. 2 consist of an instantaneous peak at zero time delay, which is a FWM signal diffracted in the direction of the probe beam and can therefore not be avoided in this experimental geometry. Additionally, a steplike change in the anisotropic transmission is observed that follows the integral over the pump-pulse intensity. This instantaneous signal, which is also observed in THz emission experiments,<sup>4</sup> is attributed to the spatial separation of electron and hole wave functions (i.e., the  $hh_{-1}$  transition) already at zero-time delay. At larger time delays the signal is dominated by a periodic modulation due to BO's. The amplitude of the oscillatory part on the order  $10^{-4}T_0$  is related

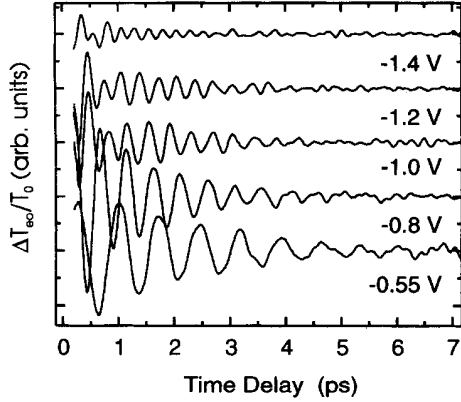


FIG. 3. Oscillatory traces of anisotropic transmission changes of the superlattice for different reverse bias.

to an internal electric field of 100 V/cm, which is in accordance with the value calculated from Eq. (2) assuming the estimated excitation density and a maximum displacement of the center of mass of the electronic wave function over some periods at lower voltages.

For a more detailed analysis of the periodic signal contribution, we omit the instantaneous part of the signal. In Fig. 3, the oscillatory contribution is shown for five different reverse bias voltages. More than ten cycles of the oscillations are clearly visible within the dephasing time. The oscillation frequency rises with increasing field, as expected from the semiclassical Bloch picture equivalent to an increase of the energetic splitting of the  $hh_{-1}$  and  $hh_0$  WS transitions. Furthermore, the amplitude drops with increasing electric fields. To interpret this behavior, three points have to be taken into consideration. (1) The decrease of the absorption strength of the  $hh_{-1}$  transitions with increasing field-induced localization. Furthermore the spectral position of the  $hh_{-1}$  transition changes. When the laser is kept at the same wavelength, the excitation density  $N$  drops at higher fields. According to Eq. (2) the polarization associated with the coherent dipole oscillation decreases. (2) The increasing localization of WS states at high electric fields leads to a reduction of the localization length  $L$ . As a consequence the amplitude of displacement [ $\langle \Delta z_e(\tau) \rangle$  in Eq. (2)] between the electronic wave packet and localized holes is reduced. (3) The finite duration of the probing pulse implies a reduced contrast in the oscillations at higher frequencies. This convolution is of minor importance for frequencies below 4 THz. The experimentally observed decrease in amplitude therefore has to be attributed to the first two points. When the absorption strength of the transitions involved is calibrated as a function of electric field, the spatial amplitude  $\langle \Delta z_e(\tau) \rangle$  of the oscillations can be determined from TEOS measurements.

In Fig. 4 the direct numerical Fourier transform of the data displayed in Fig. 3 are shown. The spectral peak positions of the Bloch frequency can be determined within an error of  $\pm 50$  GHz equivalent to a precision in the determination of the WS state splitting of  $\pm 0.2$  meV. In the WS regime, highly accurate measurements of the internal electric fields in the SL are therefore possible. This energy resolution can be obtained neither in THz emission experiments due to the limited detection bandwidth of the antennas (see, e.g., Ref. 4) nor in FWM experiments, where the frequency is

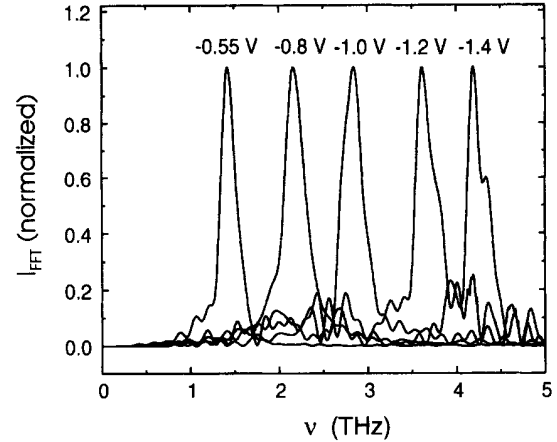


FIG. 4. Fourier transforms of time-domain signals shown in Fig. 3.

derived from the temporal distance of two<sup>2</sup> or some more<sup>3</sup> beating bumps observed within the decay of the third-order interband polarization. The spectral width of the Fourier transforms of about 260 GHz does not change significantly in the WS regime of the SL. The dephasing time of the coherent intraband polarization seems to be independent of the field applied in the WS regime. At higher fields, the Fourier spectra become slightly asymmetric towards the high energy side. A possible explanation for this behavior are inhomogeneous field distributions with a deviation of  $\pm 3\%$  from the main value within the SL. The asymmetry in the frequency domain at higher fields is also confirmed in a non-exponential decay in the time-domain data illustrated in Fig. 3. At lower fields, where an exponential decaying is observed, the numerical fit to the data gives a dephasing time of 2.8 ps, which is significantly longer than the dephasing time  $T_2$  of 1.4 ps derived from FWM experiments under *identical* excitation conditions.<sup>18</sup> We attribute the dephasing time of the FWM signal to the dephasing of excitonic wave packets. In TEOS experiments, the dephasing of the electronic wavepacket motion  $\langle \Delta z_e(\tau) \rangle$  relative to the localized holes is monitored, which is dominated by electronic intraband scattering processes alone. This distinct difference in dephasing times in the interband FWM and intraband TEOS experiments is of particular interest for the understanding of the microscopic picture of dephasing of BO's in SL's. The dephasing of BO's has been addressed recently from different aspects<sup>19,20</sup> and TEOS experiments provide firm experimental data for detailed investigations.

For a further investigation of the oscillatory contribution, we tune the applied voltage from +0.2 V to -1.9 V. The upper voltage is close to flatband (zero current) in this sample. The frequency values obtained from the Fourier transform of this data are shown in Fig. 5. We distinguish two voltage ranges. (i) Above  $-0.25$  V reverse bias, the frequency linearly depends on the voltage applied up to  $-1.9$  V. (ii) Below  $-0.25$  V down towards the flatband condition the frequency is hardly altered by the bias voltage. The first observation is in good agreement with the voltage dependence of the WS transitions involved in the beating. Slight deviations from the linear dependence can be accurately correlated to changes in the total absorption of the pump pulse, which is recorded simultaneously via the photocurrent through the sample. When the photocurrent peaks

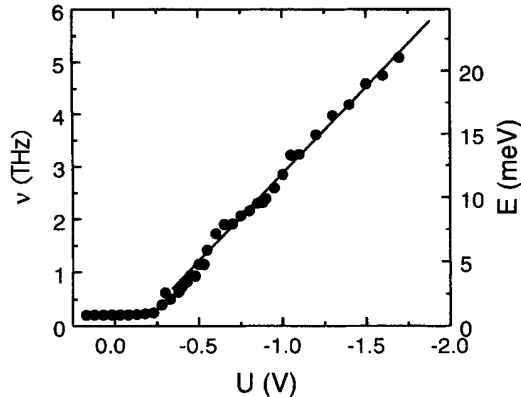


FIG. 5. Frequency of Bloch oscillations versus external bias obtained from Fourier transformation of TEOS data.

(drops), the frequency lies below (above) the linear fit due to cw accumulation of carriers partially screening the applied field.<sup>17</sup> This accumulation effect also shifts the onset of the linear field-frequency relation toward  $-0.25$  V. Without this effect, the Bloch regime is already observed at lower voltages, when the splitting of the miniband into the WS ladder becomes visible in photocurrent spectra under low excitation conditions (see, e.g., Ref. 4). The slope of the linear fit is  $(3.29 \pm 0.06)$  THz/V, which is larger than the theoretically expected value of  $ed/hl_{\text{sample}} = 2.76$  THz/V, where  $l_{\text{sample}}$  is the total intrinsic region of 999 nm including intrinsic  $\text{Al}_{0.7}\text{Ga}_{0.3}\text{As}$  buffer layers. This difference is also attributed to the screening effect, which modifies the relation between the externally applied voltage and the internal effective field.

The highest frequency observed is 5.1 THz corresponding to 21 meV. This is slightly above the theoretical maximum value for BO's in this sample, which is given by

$\nu_{\text{max}} \approx \Delta/h = 4.6$  THz assuming a calculated miniband width of 19 meV. Thus there is still absorption strength in the  $-1$  transition even when the energy splitting is larger than the calculated minibandwidth. The lowest BO frequency observed within the dephasing time in this field regime is about 300 GHz.

In the second regime below  $-0.25$  V reverse bias, the frequency changes from 210 GHz to 250 GHz only. Similar observations are made in THz experiments, although there the voltage dependence of this oscillation is even weaker than in our experiments presumably due to higher excitation densities.<sup>21</sup> The frequencies observed correspond to a beating of transitions with an energy splitting of about 1 meV, which are not resolved in cw techniques. Exciton-biexciton beats may play a crucial role in this regime. A clear interpretation, however, requires further investigation.

In conclusion, we presented an electro-optic method for the detection of coherent interband polarization associated with BO's. The amplitude, frequency, and dephasing are determined as a function of the external field. Over a wide range of applied voltages the frequency increases linearly as expected from the semiclassical picture of BO's. The amplitude of the oscillations decreases with increasing field due to increasing localization of the WS states. The dephasing time is unaffected by the electric field in the WS regime, but shows deviations from a strictly monoexponential decay at higher reverse bias. TEOS is demonstrated to be a powerful technique for an accurate determination of the frequency of BO's not accessible by other techniques.

Fruitful discussions with H.G. Roskos and H.J. Bakker are gratefully acknowledged. We thank W. Beck and R. Ott for experimental help. K. Leo is gratefully acknowledged for leading us on the track of BO research. This work was supported by the Volkswagen Stiftung and the Alfred-Krupp Stiftung.

<sup>1</sup> See, e.g., in *Optics of Semiconductor Nanostructures*, edited by F. Henneberger, S. Schmitt-Rink, and E.O. Göbel (Akademie Verlag, Berlin, 1993), and references therein.  
<sup>2</sup> J. Feldmann, K. Leo, J. Shah, D.A.B. Miller, J.E. Cunningham, S. Schmitt-Rink, T. Meier, G. von Plessen, A. Schulze, and P. Thomas, *Phys. Rev. B* **46**, 7252 (1992).  
<sup>3</sup> K. Leo, P. Haring Bolivar, F. Brüggemann, R. Schwedler, and K. Köhler, *Solid State Commun.* **84**, 943 (1992).  
<sup>4</sup> C. Waschke, H.G. Roskos, R. Schwedler, K. Leo, H. Kurz, and K. Köhler, *Phys. Rev. Lett.* **70**, 3319 (1993).  
<sup>5</sup> G.H. Wannier, *Rev. Mod. Phys.* **34**, 645 (1962).  
<sup>6</sup> F. Bloch, *Z. Phys.* **52**, 555 (1928).  
<sup>7</sup> C. Zener, *Proc. R. Soc. London Ser. A* **145**, 523 (1934).  
<sup>8</sup> L. Esaki and R. Tsu, *IBM J. Res. Dev.* **61**, 61 (1970).  
<sup>9</sup> T. Yajima and Y. Taira, *J. Opt. Soc. Jpn.* **47**, 1620 (1979).  
<sup>10</sup> G. Bastard and R. Ferreira, in *Spectroscopy of Semiconductor Microstructures*, Vol. 206 of *NATO Advanced Studies Institute, Series B: Physics*, edited by G. Fasol and A. Fasolino (Plenum, New York, 1989), p. 333.  
<sup>11</sup> S.E. Ralph, F. Capasso, and R.J. Malik, *Phys. Rev. Lett.* **63**, 2272 (1989).  
<sup>12</sup> L. Min and R.J.D. Miller, *Appl. Phys. Lett.* **56**, 524 (1990); T. Dekorsy, T. Pfeifer, W. Kütt, and H. Kurz, *Phys. Rev. B* **47**, 3842 (1993).

<sup>13</sup> G.C. Cho, W. Kütt, and H. Kurz, *Phys. Rev. Lett.* **65**, 764 (1990).  
<sup>14</sup> M. Strahlen, W. Kütt, and H. Kurz, in *Proceedings of an International Conference on VME-bus in Research*, edited by C. Eck (North-Holland, Amsterdam, 1988), p. 69.  
<sup>15</sup> A. Yariv, *Introduction to Optical Electronics* (Holt, Rinehart and Winston, New York, 1971).  
<sup>16</sup> A.V. Kuznetsov and C.J. Stanton (private communication).  
<sup>17</sup> P. Leisching, P. Haring Bolivar, W. Beck, Y. Dhaibi, F. F. Brüggemann, R. Schwedler, H. Kurz, K. Leo, and K. Köhler, *Phys. Rev. B* (to be published).  
<sup>18</sup> Since for the TEOS experiments the directly transmitted probe beam is detected, degenerate FWM can be performed simultaneously by detection of the diffracted beam. The simultaneous determination of the interband and intraband dynamics gives complete information on a three-level system.  
<sup>19</sup> A.M. Bouchard and M. Luban, *Phys. Rev. B* **47**, 6815 (1993).  
<sup>20</sup> G. von Plessen, T. Meier, J. Feldmann, E.O. Göbel, P. Thomas, K.W. Goosen, J.M. Kuo, and R.F. Kopf, *Phys. Rev. B* **49**, 14 058 (1994).  
<sup>21</sup> H.G. Roskos, in *Festkörperprobleme/Advances in Solid State Physics*, edited by R. Helbig (Vieweg, Braunschweig, in press), Vol. 34.